1992ApJ...392..647N

THE ASTROPHYSICAL JOURNAL, 392:647–652, 1992 June 20
© 1992. The American Astronomical Society. All rights reserved. Printed in U.S.A.

DYNAMO ACTION IN STRATIFIED CONVECTION WITH OVERSHOOT

ÅKE NORDLUND
Copenhagen University Observatory, Øster Voldgade 3, DK-1350 Copenhagen K, Denmark
AXEL BRANDENBURG
NORDITA, Blegdamsvej 17, DK-2100 Copenhagen Ø, Denmark; and Observatory and Astrophysical, Laboratory, University of Helsinki, Tähtitorninmäki, SF-00130 Helsinki, Finland
RICHARD L. JENNINGS
DAMTP, Silver Street, Cambridge CB3 9EW, UK
MICHEL RIEUTORD
Observatoire Midi-Pyrénées, 14 av. E. Belin, F-31400 Toulouse, France; and CERFACS, 42, Avenue Coriolis, F-31057 Toulouse, France
JUHA RUOKOLAINEN
Centre for Scientific Computing, PO Box 40, SF-02101 Espoo, Finland
ROBERT F. STEIN
Department of Physics and Astronomy, Michigan State University, East Lansing, MI 48824
AND
ILKKA TUOMINEN
Observatory and Astrophysics Laboratory, University of Helsinki, Tähtitorninmäki, SF-00130 Helsinki, Finland
Received 1991 October 15; accepted 1991 December 27

ABSTRACT

We present results from direct simulations of turbulent compressible hydromagnetic convection above a stable overshoot layer. Spontaneous dynamo action occurs followed by saturation, with most of the generated magnetic field appearing as coherent flux tubes in the vicinity of strong downdrafts, where both the generation and destruction of magnetic field is most vigorous. Whether or not this field is amplified depends on the sizes of the magnetic Reynolds and magnetic Prandtl numbers. Joule dissipation is balanced mainly by the work done against the magnetic curvature force. It is this curvature force which is also responsible for the saturation of the dynamo.

Subject headings: convection — MHD — stars: interiors — turbulence

1. INTRODUCTION

Understanding the spontaneous generation of magnetic fields in astrophysical systems is a classical problem of theoretical physics. The magnetic fields of the Earth and the Sun are nearby examples, but magnetic fields are ubiquitous in most planets, stars, and indeed galaxies. Some kind of turbulent dynamo process is widely believed to be responsible (Larmor 1919; Parker 1979) but, although examples of working dynamos exist (e.g., Gilman & Miller 1981; Glatzmaier 1985, Meneguzzi & Pouquet 1989; Kida, 1991), the details of the amplification process remain uncertain.

A turbulent dynamo amplifies a seed magnetic field by converting kinetic energy from the turbulent flow into magnetic energy. It appears likely that dynamo action occurs in any "sufficiently turbulent" plasma, where a simple seed field is repeatedly mapped by a complicated flow into an increasingly intricate pattern. In such a flow even the slightest diffusion leads to changes in the field topology which are virtually irreversible. The lengthening of field lines corresponds to an increase of field strength with time, and the cumulative effect of such mappings may be the essence of dynamo action in a turbulent plasma. A simple example of cumulative effects is the "stretch-twist-fold" dynamo (Vainshtein & Zeldovich 1972).

In this paper, we study a model situation where the ingredients of a turbulent dynamo are present; turbulent motions in a weakly diffusive electrically conducting plasma. The motions are driven by the convective instability of a gravitationally stratified layer heated from below. The convectively unstable layer is situated on top of a layer which, because of a larger heat conductivity, is convectively stable, similar to the radiative zone below a stellar envelope convection zone.

We do not attempt to model global dynamo action in a spherical shell. Such calculations are exceedingly demanding in computing power, since spatial scales ranging from global down to a fraction of a scale height must be represented. We do, however, include rotation in the model, by including the Coriolis force corresponding to rotation of the local coordinate system with constant rotation speed. By choosing a Rossby number (ratio of rotational to convective times scales) near unity, we achieve a set-up where the relative importance of advective and rotational effects is similar to that in the solar convection zone.

The model is described in more detail in the following section. In § 3 we describe the qualitative and quantitative behavior of the convective motions and the magnetic field in the model. We find that weak seed fields are indeed greatly amplified with time, and in § 4 we discuss whether or not this is due to dynamo action.

2. THE MODEL

We consider a local Cartesian region of depth $2d$, with a convectively unstable upper half ($0 < z < d$) and a convectively stable lower half ($d < z < 2d$). Convective stability in the lower half is obtained by assuming a 3 times larger radiative conductivity $\mathscr{K}$ there, as did Hurlburt, Toomre, & Massaguer (1986). Such a two-layer configuration permits richer topologies and

© American Astronomical Society • Provided by the NASA Astrophysics Data System

1992ApJ...392..647N

gives the dynamo more freedom than a single layer. Further, evidence suggests that the solar dynamo works deep in the convective zone or perhaps in the overshoot region, since at shallower locations magnetic buoyancy is expected to cause the generated flux to rise to the surface too rapidly (Parker 1975). The vertical extent of the domain spans four pressure scale heights. By adjusting the angle at which the rotation and gravity vectors $\boldsymbol{\Omega}$ and $\boldsymbol{g}$ are inclined, we can locate this volume at any latitude in a spherical shell. The results presented here are for a latitude of 30° south.

Interactions between fluid motions $\boldsymbol{u}$ and magnetic fields $\boldsymbol{B}$ are governed by the induction equation, together with equations for the conservation of momentum, energy, and mass:

$$\frac{\partial \boldsymbol{B}}{\partial t} = \text{curl}\,(\boldsymbol{u} \times \boldsymbol{B}) + \eta \nabla^2 \boldsymbol{B}\,, \tag{1}$$

$$\rho \frac{D\boldsymbol{u}}{Dt} = -\nabla p + \rho \boldsymbol{g} - 2\boldsymbol{\Omega} \times \rho \boldsymbol{u} + \boldsymbol{J} \times \boldsymbol{B} + \text{div}\,(2\nu\rho \boldsymbol{S})\,, \tag{2}$$

$$\rho \frac{De}{Dt} = -p\ \text{div}\ \boldsymbol{u} + \nabla(\mathcal{K}\nabla e) + 2\nu\rho \boldsymbol{S}^2 + \frac{\boldsymbol{J}^2}{\sigma}\,, \tag{3}$$

$$\frac{D \ln \rho}{Dt} = -\text{div}\ \boldsymbol{u}\,. \tag{4}$$

Here, $S_{ij} = \frac{1}{2}(\partial_j u_i + \partial_i u_j - \frac{2}{3}\delta_{ij}\text{div}\ \boldsymbol{u})$, ν is the kinematic viscosity, which is assumed to be constant, $\boldsymbol{J} = \text{curl}\ \boldsymbol{B}/\mu_0$ is the electric current, σ the electrical conductivity, $\eta = 1/(\mu_0 \sigma)$ the magnetic diffusivity (assumed constant), and all other quantities have their usual meaning. The model parameters are a Prandtl number of 0.2, a Taylor number of 10^5 and a Rayleigh number of 10^6, which is $\sim$50 times supercritical (for definitions, see Brandenburg et al. 1990). An important parameter is the magnetic Prandtl number $\text{Pr}_M = \nu/\eta$, which is varied between $\frac{1}{4}$ and 20.

We adopt boundary conditions that are mathematically convenient, yet physically plausible. The lower and upper boundaries ($z = 0, 2d$) are impenetrable stress-free perfect conductors. A constant radiative flux is imposed at the bottom and the top is cooled isothermally. All quantities are assumed to be periodic in the horizontal directions. Numerical solutions are obtained on a grid of 63^3 points, using a modified version of the code by Nordlund & Stein (1989).

3. MODEL BEHAVIOR

Before inserting any magnetic field we allow the convection to reach a well-developed state. The flow is irregular, yet large-scale features are distinguishable, notably strong narrow downdrafts in the form of tornado-like vortex tubes that swish to and fro. Gravity waves are excited (Hurlburt, Toomre, & Massaguer 1986), which shake these downdrafts, especially if they extend into the overshoot region. The flow has coherent vortex tubes and an energy spectrum compatible with $k^{-5/3}$ in the inertial range, both of which occur in simulations of isotropic turbulence (e.g., She, Jackson, & Orszag 1990; Vincent & Meneguzzi 1991).

We then introduce a seed horizontal magnetic field which has the property that its average is zero, i.e., $\int \boldsymbol{B}\,dV = \boldsymbol{0}$. There is a rapid concentration of magnetic flux into thin elongated tubes. Vortex tubes associated with downdrafts are comparatively straight and vertical, while tubes (both magnetic and vortex) at other locations are typically curved.

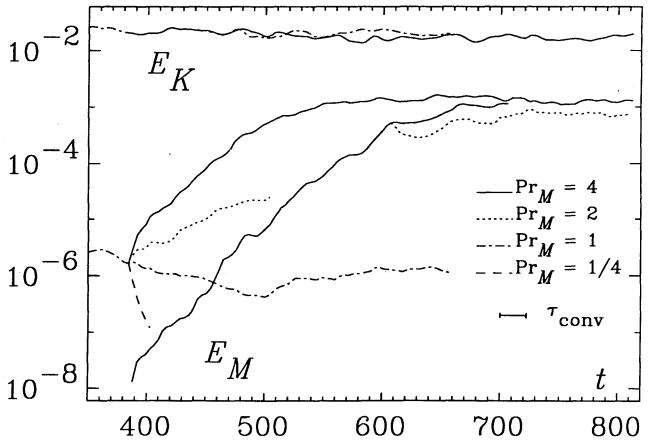

FIG. 1.—The exponential growth of magnetic energy E_M and subsequent saturation (*lower two solid curves*, $\text{Pr}_M = 4$). A reduction by a factor 10^2 in the seed field's strength gives the same saturation energy (*lower solid curve*, $\text{Pr}_M = 4$). For smaller Pr_M there is no growth (*lower dotted-dashed curve*, $\text{Pr}_M = 1$). Note that in the case of $\text{Pr}_M = 4$ there is a noticeable change in the flow's kinetic energy E_K (see *upper solid and dotted-dashed curves* for $\text{Pr}_M = 4$ and 1, respectively).

In Figure 1 we summarize the magnetic field evolution for various values of Pr_M over $\sim$400 time units [time is measured in units of $(d/g)^{1/2}$] or nearly 20 turnover times (τ_{conv}). The Reynolds number in all cases is $\sim$300. For $\text{Pr}_M > 1$ there is an initial exponential growth in magnetic energy $E_M = \int \boldsymbol{B}^2/(2\mu_0)dV$, with an e-folding time close to τ_{conv} for $\text{Pr}_M = 4$ and close to $2\tau_{\text{conv}}$ for $\text{Pr}_M = 2$. Small values of Pr_M, e.g., $\frac{1}{4}$, lead to rapid decay. This is consistent with Batchelor's (1950) argument that a magnetic field in a turbulent fluid will be amplified if $\text{Pr}_M > 1$. We note, however, that using a larger Prandtl number raised the critical value of Pr_M above unity.

In Figure 2*a* (Plate 3) we visualize the vorticity and the magnetic field vectors, while Figure 2*b* (Plate 3) shows that vortex tubes are associated with a reduction in pressure. The pressure reduction associated with the magnetic flux tubes is, however, insignificant in the picture.

The Lorentz force is responsible for the saturation (suppressing it leads to continued growth). A decomposition of $\boldsymbol{J} \times \boldsymbol{B}$ into its pressure, tension, and curvature forces is as follows (see Priest 1982):

$$\begin{aligned} &\text{Pressure gradient force:} && -\frac{1}{2\mu_0}\nabla \boldsymbol{B}^2\,, \\ &\text{tension force:} && \frac{1}{\mu_0}\hat{\boldsymbol{B}}[\hat{\boldsymbol{B}} \cdot (\boldsymbol{B} \cdot \nabla \boldsymbol{B})]\,, \\ &\text{curvature force:} && \frac{1}{\mu_0}\{\boldsymbol{B} \cdot \nabla \boldsymbol{B} - \hat{\boldsymbol{B}}[\hat{\boldsymbol{B}} \cdot (\boldsymbol{B} \cdot \nabla \boldsymbol{B})]\}\,, \end{aligned} \tag{5}$$

where $\hat{\boldsymbol{B}}$ is the unit vector in the direction of $\boldsymbol{B}$. From various additional runs, summarized in Figure 3, we conclude that magnetic pressure does not limit the field growth and that magnetic tension has only a small effect. It is primarily the curvature force that causes saturation of the dynamo. The final magnetic energy is independent of the initial field strength, but depends on Pr_M (see Fig. 1).

4. DYNAMO ACTION

Dynamo action means that an arbitrarily weak seed magnetic field is exponentially amplified and maintained against

© American Astronomical Society • Provided by the NASA Astrophysics Data System

1992ApJ...392..647N

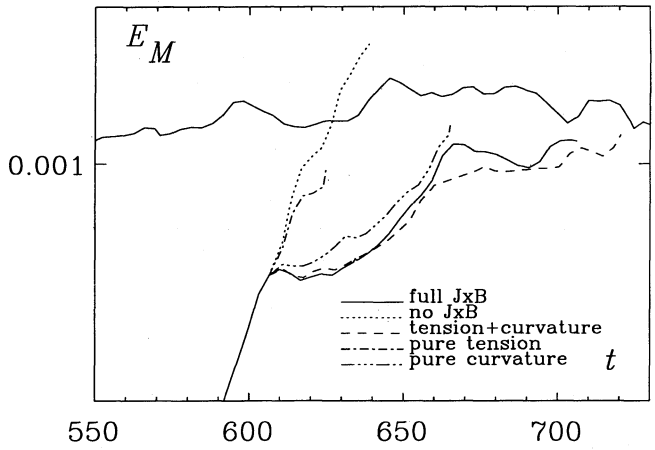

FIG. 3.—The effect of various feedback terms on the saturation of the dynamo. Neglecting the Lorentz force leads to continued exponential growth (*dotted line*). Saturation is mainly due to the curvature force (*triple-dot-dashed and dashed curves*).

Joule dissipation. For a large-scale field, e.g., $B_y \sim \sin(\pi z/d)$, the e-folding time for Joule dissipation is, in the absence of any motions, $d^2/(\pi^2\eta) \approx 2000$ time units. Since our simulation covers only a fraction of this (global) diffusion time one might argue that the field amplification in Figure 1 is just a transient, and that the field might eventually decay. In subsection 4.2 below, we show that the relevant time scale is much shorter than $d^2/(\pi^2\eta)$. First, however, we discuss why the concentration of field via flux expulsion is not responsible for the amplification of E_M.

4.1. *Flux Expulsion*

As an instructive example, where dynamo action is known to be impossible, we present in Figure 4 the magnetic energy's evolution for for a two-dimensional model with the same parameters as in the three-dimensional cases and $\mathrm{Pr}_M = 4$. For a limited time, the initial stretching of flux surfaces leads to an increase of the field strength and the total magnetic energy, but after less than a turnover time the field starts to decay with an e-folding time of $\sim\frac{1}{2}\tau_{\mathrm{conv}}$. This is independent of the initial field strength, unless the initial field is strong enough for the Lorentz force to be significant, in which case expulsion can take much longer (Cattaneo & Vainshtein 1991). Eventually, the decay slows down as the field is expelled from the convection zone into the overshoot region (see the two boxes inset in Fig. 4) where the motions are too weak to enhance Joule dissipation.

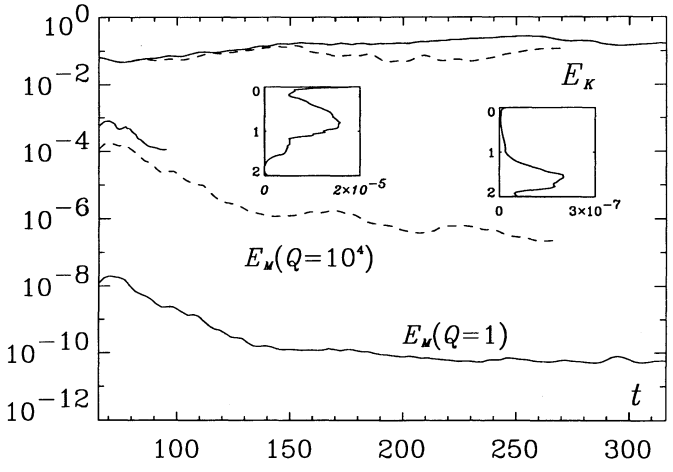

FIG. 4.—Evolution of energy in a two-dimensional model for two different initial magnetic field energies (measured by the Chandrasekhar number Q). The insets show the vertical distribution of the horizontally averaged magnetic energy density for the run with $Q = 10^4$ at $t = 102$ and $t = 269$. Note that after some time significant magnetic energy only remains in the stably stratified overshoot region.

In two-dimensional convection cells, the field tends to be expelled from the interior of cells into layers with stagnant flow along boundaries (see Weiss 1990). As a consequence, the field strength increases but only because the filling factor decreases, with the total magnetic energy being inversely proportional to the filling factor (neglecting diffusion). In principle, field amplification is similarly possible in three dimensions, that is, an initially diffuse field can be concentrated into a small subvolume. Since magnetic structures show no tendency to shorten in this experiment, the maximum possible increase of magnetic energy due to flux expulsion is proportional to the ratio of the magnetic fields initial to final cross-sectional area. With the prescribed initial seed field and numerical resolution, this ratio is at most ~ 100 in our model, and therefore flux explusion cannot explain a growth of the magnetic energy over five orders of magnitude. From the magnetic induction equation and our choice of boundary conditions, no growth of the average field $\int \boldsymbol{B}\,dV$ is possible in our model. Note, however, that the property $\int \boldsymbol{B}\,dV = \boldsymbol{0}$ does not exclude the formation of large-scale field belts. We wish to stress that the absence of any average field distinguishes our model from studies of magnetoconvection, where a total magnetic flux is imposed and field amplification occurs due to a concentration of the average field.

4.2. *The Flow of Energy*

Joule dissipation is important in the dynamo process, with changes in the resistivity producing immediate changes in the evolution of the magnetic energy. Raising the resistivity above a critical value causes a decay of the magnetic field, and the larger the resistivity the more rapid the decay. This is understandable as a balance between kinetic energy being converted into magnetic energy and magnetic energy being converted into heat by Joule dissipation. If, for a given level of magnetic field energy, the Joule dissipation is larger than the rate of conversion of kinetic energy, the field energy decays, if not, it increases.

From the exponential behavior of the magnetic energy (Fig. 1), we conjecture that the growth and decay processes are both proportional to the instantaneous magnetic field energy. Apart from geometrical details, the Lorentz force is proportional to the magnetic energy density divided by a characteristic structure size, while the Joule dissipation is proportional to the magnetic energy density divided by the *square* of a characteristic structure size. The exponential behavior is consistent with an evolution in which the size of magnetic structures varies only slightly, but the magnetic field strength changes. An examination of the actual distribution of magnetic fields in the model confirms that this is indeed the case. Most of the magnetic energy is in the form of long thin flux tubes, with a balance struck between thinning due to stretching and thickening by diffusion; the characteristic size of flux tubes do not change during the growth phase.

© American Astronomical Society • Provided by the NASA Astrophysics Data System

1992ApJ...392..647N

The ratio of total magnetic energy to the rate of total Joule dissipation,

$$\frac{E_M}{Q_{\rm Joule}} = \frac{1}{2\eta}\frac{\int \boldsymbol{B}^2 dV}{\int \mu_0^2 \boldsymbol{J}^2 dV} = \tau_M\,, \qquad (6)$$

is the time scale over which magnetic energy is destroyed and replenished. During amplification τ_M increases, before leveling off at a value of ~ 6 time units in the saturated phase of our simulation. A characteristic dissipation length scale λ_M may be defined as $\lambda_M^2 = 2\tau_M \eta$, which is the magnetic analogue of the Taylor microscale, and is, in our case, of the order of the mesh size.

The slight decrease in E_M after saturation is due to a relaxation on a slow, thermal time scale. Apart from this the various energy reserviors, and the transfer rates between them remain statistically stationary during the magnetically saturated part of our experiment. Since this saturation part is far longer than τ_M we conclude that the magnetic field is maintained by a dynamo. Revelant at this stage is the work of Cattaneo, Hughes, & Weiss (1991), in which it is proposed that the important decay time scale in turbulent dynamos is τ_M multiplied by a model-dependent "safety factor." According to their prescription the safety factor in our simulation is $O(1)$, thus substantiating our claim of dynamo action.

The change of magnetic energy in each horizontal layer is governed by the equation:

$$\frac{\partial}{\partial t}\left\langle \frac{\boldsymbol{B}^2}{2\mu_0}\right\rangle = -\frac{\partial}{\partial z}\left\langle \frac{\boldsymbol{E}\times\boldsymbol{B}}{\mu_0}\right\rangle - \langle \boldsymbol{u}\cdot(\boldsymbol{J}\times\boldsymbol{B})\rangle - \langle \boldsymbol{J}^2/\sigma\rangle\,, \qquad (7)$$

where the angular parentheses denote horizontal averages, $\boldsymbol{E} = -\boldsymbol{u}\times\boldsymbol{B} + \boldsymbol{J}/\sigma$ is the electric field, and $-\boldsymbol{u}\cdot(\boldsymbol{J}\times\boldsymbol{B})$ is the work done against the Lorentz force. Figure 5 displays temporal averages of the vertical dependence of various terms in equation (7). The maximum of magnetic energy is slightly below the interface at $z = 1$. The work done by the Lorentz force is negative, corresponding to a transfer of energy from the flow (kinetic) into magnetic energy. Most of this work is contributed by the downward flow (*dashed line*).

The divergence of the horizontally averaged Poynting flux $\langle \boldsymbol{E}\times\boldsymbol{B}/\mu_0\rangle$ is positive in the unstable layer and negative in the stable layer. Thus, on average, the Poynting flux transports magnetic energy from the unstable layers down into the stable layers by advection of the field in downdrafts. Note, however, that the average of the divergence of the Poynting flux in the *ascending* flow is negative in the lower part of the unstable zone too; this is a manifestation of magnetic energy being advected into the ascending flow.

In the last panel of Figure 5 we compare the rate of Joule dissipation with various contributions to the work done against the Lorentz force. All three components of the Lorentz force, the magnetic pressure gradient, the tension force and the curvature force, contribute to dynamo action in the convectively unstable region. We note that sites of strong field generation coincide with sites of strong field dissipation, the two effects being almost equal and opposite. This is to be expected in a saturated state of the dynamo if the rate of transport of magnetic energy (divergence of the Poynting flux) is small relative to the rate of Joule dissipation (see eq. [7]).

The work done against the curvature force is primarily responsible for the increase in magnetic energy. Saturation occurs when the curvature force is strong enough to force flux tubes through the fluid, instead of stretching and bending them further. The work done by the fluid *on the magnetic field* is given by the Lorentz force term of equation (7). This differs from the work done by the fluid on the flux tube and its immediate surroundings, which also includes work going into the viscous dissipation associated with the motion of the plasma around the flux tube. At saturation, all the work done by the fluid on the magnetic field is, on the average, converted into Joule heat and none is left to increase the magnetic energy.

Figure 6 shows the global balance between Joule dissipation and work done against the Lorentz force. During the growth phase, the work and the dissipation differ by a small but con-

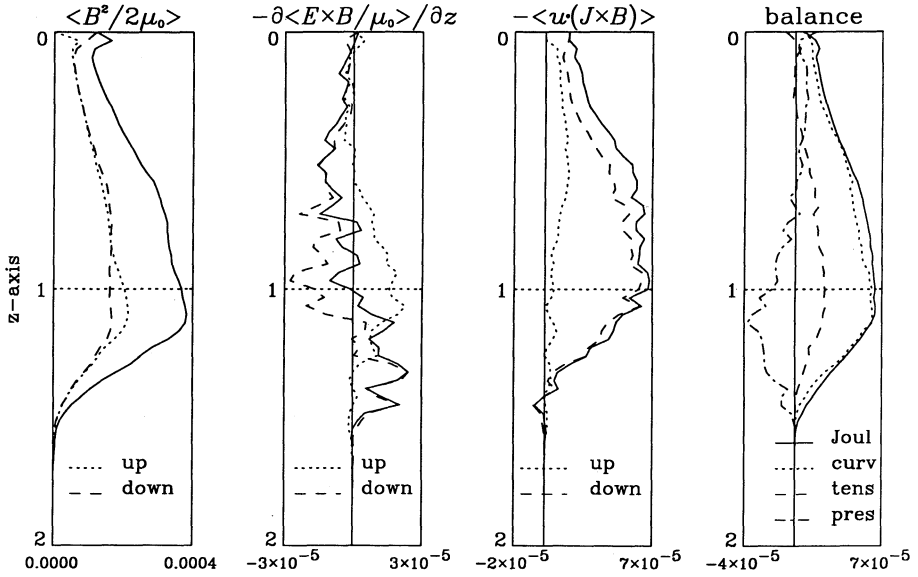

FIG. 5.—The first three panels show vertical profiles of magnetic energy density, divergence of the Poynting flux, and work done by the Lorentz force. Dashed and dotted lines give, respectively, the contributions from regions with upward and downward flow. In the last panel the rate of Joule dissipation is compared with the work done by the curvature force (*dotted curve*), tension force (*dashed curve*), and pressure gradient force (*dashed-dotted curve*).

© American Astronomical Society • Provided by the NASA Astrophysics Data System

1992ApJ...392..647N

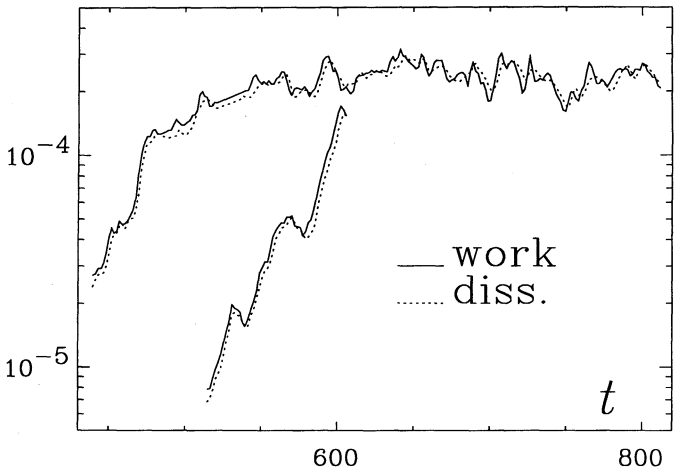

FIG. 6.—The global balance between work done against the Lorentz force (*solid curve*) and the Joule dissipation (*dashed curve*). The two sets of curves correspond to cases with different initial seed field (see Fig. 1).

sistently positive amount. In the saturated phase the difference between the work dissipation fluctuates around zero. Note that the amplitude of the fluctuations of the work exceeds that of the dissipation, and that fluctuations in the work typically lead similar, lower amplitude fluctuations of the dissipation. Also note the episodic character of the exponential growth, which is more evident in the work than in the magnetic energy (see Fig. 1).

4.3. *Qualitative Nature of the Dynamo*

A video animation shows a powerful spinning vortex tube that winds up magnetic flux tubes like spaghetti around a fork. A snapshot showing the spiraling of tubes as a result of this swirling process is shown in Figure 7 (Plate 4). The upper part of the spiral is pushed downwards and folded onto the lower part. The descending flow diverges as it encounters the interface at $z = 1$. Some of the magnetic field is dragged along the interface and caught in an updraft, but soon returns in another downdraft having experienced further folding.

In our model setup, this chain of events is particularly simple and understandable. The powerful downdrafts are created by the gravitational stratification (see Stein & Nordlund 1989) and are set in systematic rotation by the Coroilis force. Field lines caught in this motion are twisted, folded, and piled up against the interface with the convectively stable layers below the convection zone, into which convective motions do not penetrate very far. Dissipation enables the piled-up fields to partially merge. The interface forces the descending gas to expand, which stretches the magnetic field lines as they are advected away from the downdraft. Stretched loops of magnetic field are transported by the ascending flow, recaptured by downdrafts and reprocessed into a situation with similar topology but increased magnetic field strength.

The process described above is qualitatively similar to the stretch-twist-fold dynamo sequence (Vainshtein & Zeldovich 1972) for closed flux tubes. In our case, magnetic field lines are not closed, and the concept of the flux tube is only valid locally.

Amplification continues until the Lorentz force is strong enough to resist the flow. Viscous drag and magnetic dissipation are key factors in this balance between amplification and dissipation. The relative strength of these effects is measured by Pr_M. Increasing viscosity increases the viscous drag on the flux tube. Increasing resistivity decreases the drag, by allowing plasma to diffuse through the flux tube. For large Pr_M, a sufficiently small magnetic flux tube is tightly coupled to the surrounding flow by viscous forces, while at the same time diffusion of the magnetic field is insignificant. Such tubes are efficient participants in the dynamo process described above, and correspond to high values of E_M at saturation. As Pr_M decreases because viscous effects are reduced or because resistive diffusion is increased, the plasmas grip upon magnetic flux tubes weakens. This results in the dynamo saturating at a lower value of E_M. If Pr_M is too small (and η is too large), there is no dynamo.

We emphasize that we expect the dynamo efficiency at constant $\mathrm{Pr}_M = \nu/\eta$ to also depend on the magnitude of ν. In addition to controlling the viscous drag on flux tubes, ν also influences the vigor of the convective flow. In particular, the strength of the narrow downdrafts increases with decreasing ν. Hence, we expect the dynamo efficiency at constant Pr_M to increase with decreasing ν. Even in the limit of vanishing viscosity, there is a (turbulent) drag on flux tubes, which should allow dynamo action. Thus, for sufficiently small η, dynamo action might be possible in the limit $\mathrm{Pr}_M \to 0$.

5. CONCLUSIONS

We may summarize a qualitative scenario of our dynamo simulation as follows: dynamo amplification of a seed field occurs because of the continual stretching, twisting, and folding of magnetic field lines by the convective flow. In our experiment, concentrated spinning downdrafts result as a consequence of stratification and rotation. Most of the work done against the Lorentz force occurs when magnetic fields are sucked into and wound round these downdrafts. The largest component of this work is done against curvature forces, as magnetic flux tubes are bent and stretched. Saturation is reached when the curvature force is strong enough to force the magnetic flux to diffuse (slip) through the plasma. At this point, all work against the curvature force is transformed into Joule heating.

Fundamentally, there is an irreversible transfer of energy, initially from the ordered supply of thermal energy to kinetic energy associated with rotating convection. Then from kinetic to magnetic energy as the motions wind up the field, and finally from magnetic to thermal energy via Joule dissipation. Most of the magnetic energy is in the form of magnetic flux tubes, and thus the characteristic dissipation time of the magnetic field energy is the dissipation time of individual flux tubes.

Studying turbulent dynamo action in a relatively simple geometry such as this, has the advantage that the individual processes are easily identified. It was not our intention to model a realistic stellar dynamo. Stellar dynamos probably operate on a global scale, with differential rotation as an important cause of field line stretching. Three-dimensional spherical simulations are necessary to study such dynamos. Even so, the fundamental mechanisms discussed here are likely to be part of real stellar dynamos as well.

Most of the computations were carried out on the Cray-XMP/432 of the Centre for Scientific Computing, Espoo, Finland. Additional runs at a resolution of 127^3 meshpoints were performed on the Cray-2 at CCVR (Centre de Calcul Vectoriel pour la Recherche), Palaiseau, France. R. L. J. and R. F. S. were funded by SERC, and NASA grant NAGW-1695 respectively, while Å, N. acknowledges support from the Danish Natural Science Research Council and the Danish Space Board.

© American Astronomical Society • Provided by the NASA Astrophysics Data System

1992ApJ...392..647N

REFERENCES

Batchelor, G. K. 1950, Proc. Roy. Soc. Lond. A, 201, 405
Brandenburg, A., Nordlund, Å., Pulkkinen, P., Stein, R. F., & Tuominen, I. 1990, A&A, 232, 277
Cattaneo, F., Hughes, D. W., & Weiss, N. O., 1991, MNRAS, 253, 479
Cattaneo, F., & Vainshtein, S. I. 1991, ApJ, 376, L21
Gilman, P. A., & Miller, J. 1981, ApJ, 46, 211
Glatzmaier, G. A. 1985, Geophys. Astrophys. Fluid Dyn., 31, 137
Hurlburt, N. E., Toomre, J., & Massaguer, J. M. 1986, ApJ, 311, 563
Kida, S., Yanase, S., & Mizushima, J. 1991, Phys. Fluids A, 3, 457
Larmor, J. 1919, Rep. Brit. Assoc. Adv. Sci., 159
Meneguzzi, M., & Pouquet, A. 1989, J. Fluid Mech. 205, 297
Nordlund, Å., & Stein, R. F. 1989, in Solar and Stellar Granulation, ed. R. Rutten & G. Severino, NATO ASI Ser., 263, 453
Parker, E. N. 1975, ApJ, 198, 205
———. 1979, Cosmical Magnetic Fields (Oxford: Clarendon)
Priest, E. R. 1982, Solar Magnetohydrodynamics (Dordrecht: Reidel), 91
She, Z.-S., Jackson, E., & Orszag, S. A. 1990, Nature, 344, 226
Stein, R. F., & Nordlund, Å, 1989, ApJ, 342, L95
Vainshtein, S. I., & Zeldovich, Ya. B. 1972, Soviet, Phys.—Uspekhi, 15, 159
Vincent, A., & Meneguzzi, M. 1991, J. Fluid Mech., 225, 1
Weiss, N. O. 1990, Comp. Phys. Rep. 12, 233

© American Astronomical Society • Provided by the NASA Astrophysics Data System

1992ApJ...392..647N

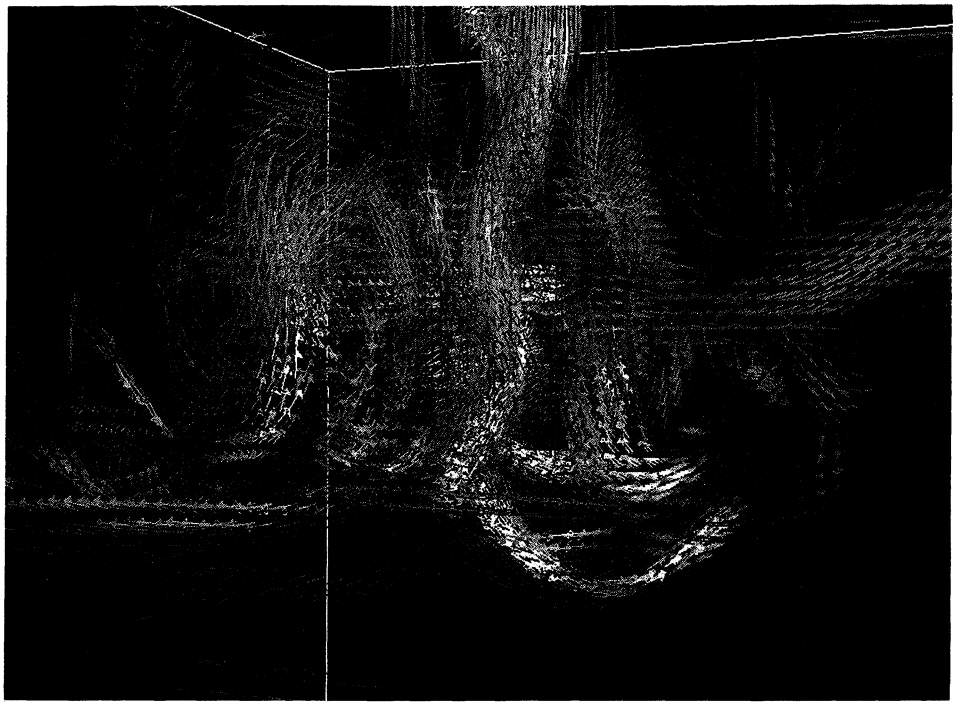

FIG. 2*a*

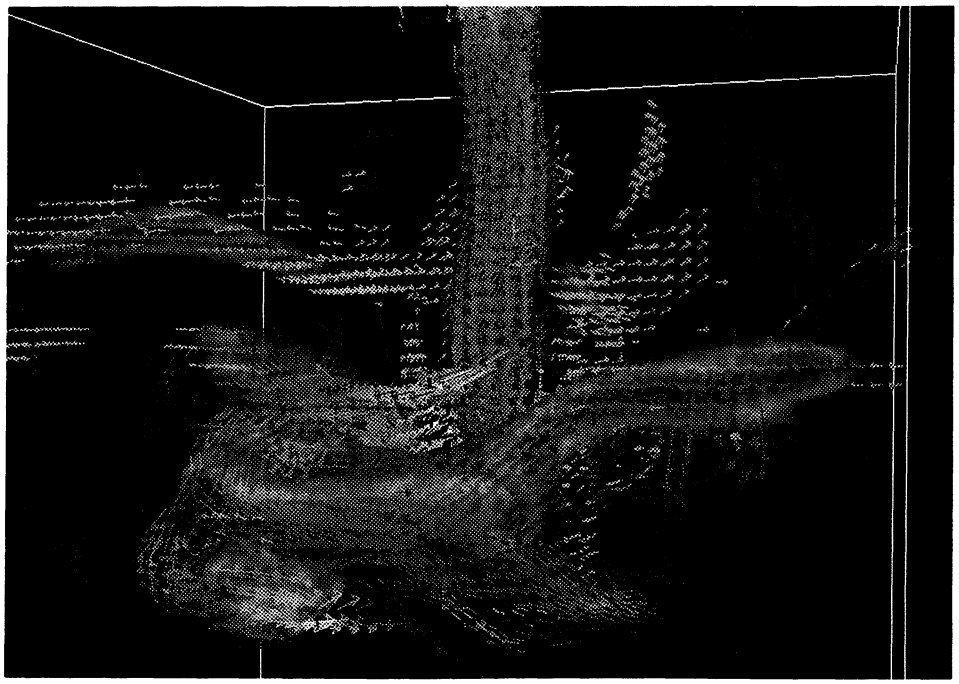

FIG. 2*b*

FIG. 2.—(*a*) Magnetic field vectors in yellow (strongest) and red (less strong) together with vorticity vectors in gray. Only vectors of vorticity and magnetic field above a certain threshold are plotted, and these dominant vectors occur in the form of tubes. The lower half of the box is stable to convection. Near the base of the convection zone the magnetic tubes are horizontally oriented and form a sharp base resembling a Cumulus cloud. In the bulk of the convection zone magnetic tubes are predominantly vertical. (*b*) Transparent surfaces of constant (negative) pressure fluctuation (*blue*) together with vorticity and magnetic field vectors. Note that pressure surfaces line up with vorticity tubes but not with magnetic flux tubes.

© American Astronomical Society • Provided by the NASA Astrophysics Data System

1992ApJ...392..647N

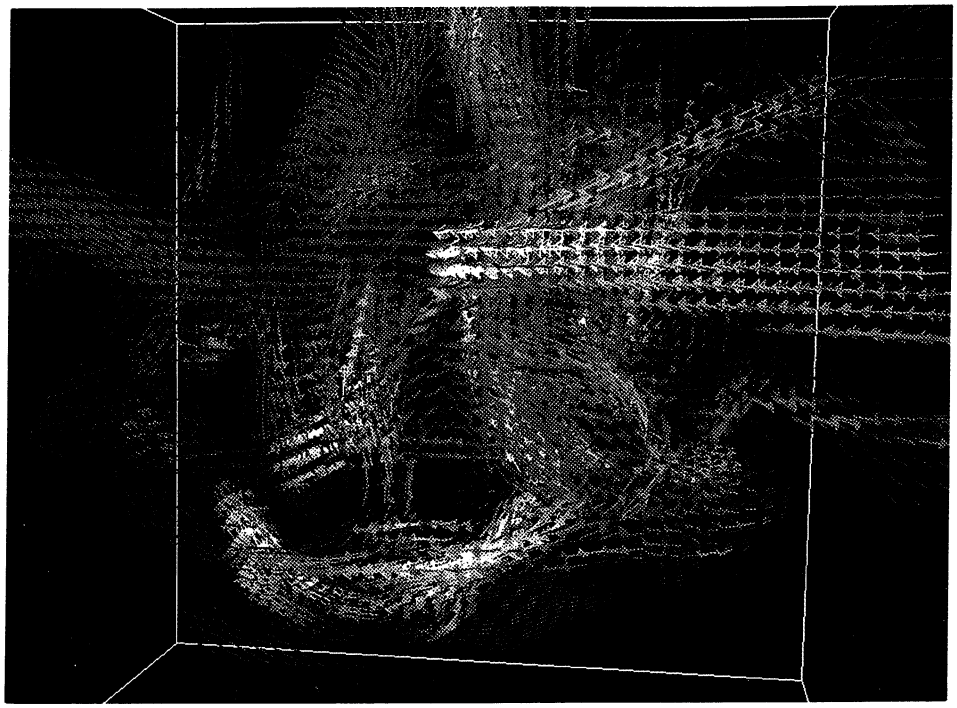

FIG. 7*a*

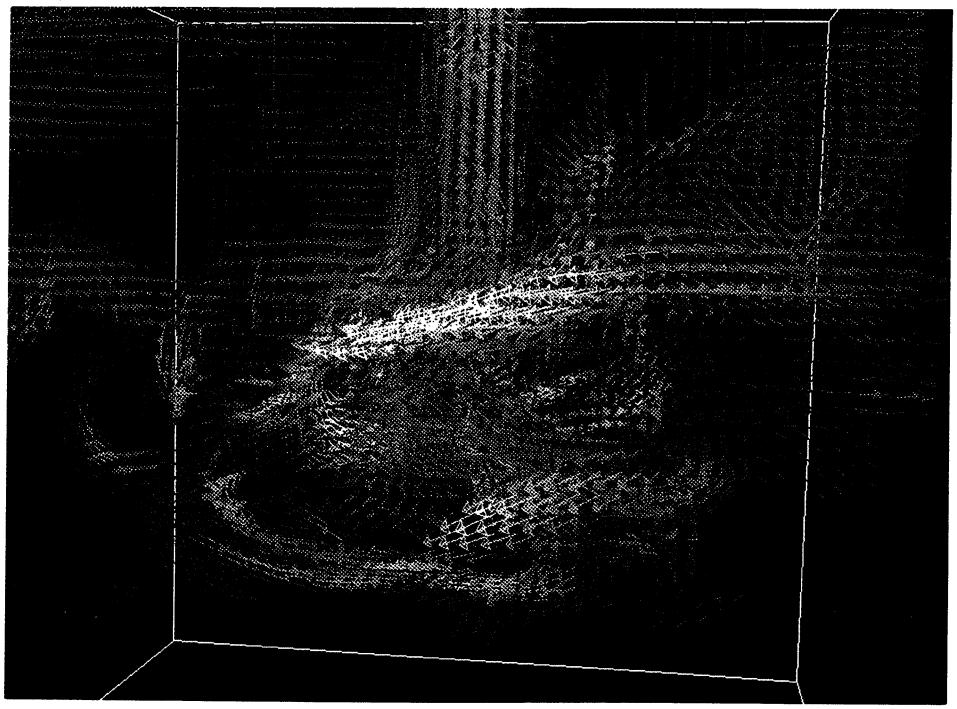

FIG. 7*b*

FIG. 7.—(*a*) Twisting and folding of magnetic flux tubes (yellow) around a vortex tube (gray) located in a downdraft. $Pr_M = 4$, $t = 721$. Flux tubes of the same orientation are pushed together. (*b*) The same as (*a*), but at $t = 725$. Note that the upper part of the spiral is pushed downward.

© American Astronomical Society • Provided by the NASA Astrophysics Data System